

**An Efficient and Accurate Algorithm for Computing Grid-Averaged Solar  
Fluxes for Horizontally Inhomogeneous Clouds**

Zhonghai Jin, Andrew Lacis

NASA Goddard Institute for Space Studies, New York, NY 10025

Corresponding author address:

Zhonghai Jin

NASA Goddard Institute for Space Studies

2880 Broadway, New York, NY 10025

email: Zhonghai.jin@nasa.gov

1    **Abstract**

2  
3       A computationally efficient method is presented to account for the horizontal cloud  
4       inhomogeneity by using a radiatively equivalent plane parallel homogeneous (PPH) cloud. The  
5       algorithm can accurately match the calculations of the reference (rPPH) independent column  
6       approximation (ICA) results, but use only the same computational time required for a single  
7       plane parallel computation. The effective optical depth of this synthetic sPPH cloud is derived by  
8       exactly matching the direct transmission to that of the inhomogeneous ICA cloud. The effective  
9       scattering asymmetry factor is found from a pre-calculated albedo inverse look-up-table that is  
10      allowed to vary over the range from -1.0 to 1.0. In the special cases of conservative scattering  
11      and total absorption, the synthetic method is exactly equivalent to the ICA, with only a small bias  
12      (about 0.2% in flux) relative to ICA due to imperfect interpolation in using the look-up tables. In  
13      principle, the ICA albedo can be approximated accurately regardless of cloud inhomogeneity.

14      For a more complete comparison, the broadband shortwave albedo and transmission calculated  
15      from the synthetic sPPH cloud and averaged over all incident directions, have the RMS biases of  
16      0.26% and 0.76%, respectively, for inhomogeneous clouds over a wide variation of particle size.

17      The advantages of the synthetic PPH method are that (1) it is not required that all the cloud  
18      subcolumns have uniform microphysical characteristic, (2) it is applicable to any 1D radiative  
19      transfer scheme, and (3) it can handle arbitrary cloud optical depth distributions and an arbitrary  
20      number of cloud subcolumns with uniform computational efficiency.

21      **Keywords:** cloud inhomogeneity, radiative transfer, solar radiation.

1     **1. Introduction**

2           Clouds have very important effect on the Earth's radiation budget of the atmosphere, thus  
3       making clouds one of the fundamental issues in the study and modeling of the climate. Accurate  
4       computation of radiative fluxes and absorption in clouds is needed to assess their impact on  
5       climate, but rigorous radiative transfer computations (e.g., Hansen and Travis, 1974) are only  
6       feasible in the framework of plane-parallel homogeneous (PPH) geometry. In contrast, surface  
7       and space observations show clouds to be intrinsically inhomogeneous. Even stratus clouds that  
8       appear to be uniform, are not actually homogeneous (e.g., King et al., 2013; Oreopoulos and  
9       Cahalan, 2005; Zhang et al., 2019, Madhavan et al., 2016), and no terrestrial cloud can adhere  
10      strictly to the horizontally unbounded PPH assumption.

11          It is well known that simply using the average value of the optical depth in PPH radiative  
12       transfer calculations for a horizontally inhomogeneous cloud field will tend to overestimate the  
13       reflectivity and underestimate the transmission (Cahalan et al., 1994a; Carlin et al., 2002; Baum  
14       et al., 2004). To address this problem, Cahalan et al. (1994a) employed the simple expedient of  
15       an effective thickness approach (ETA), where ETA utilizes an effective cloud optical thickness  
16       in the radiation computation that is smaller than the PPH thickness. However, the ETA reduction  
17       factor has to be determined empirically and this method holds only for a rather narrow range of  
18       optical depths and solar zenith angles (Barker, 1996).

19          Hogan et al. (2016) presented a method to approximate the 3D horizontal inhomogeneity  
20       effects by adding extra terms to the two-stream equations to represent lateral transport between  
21       clear and cloudy regions. The cloud inhomogeneity in this method is simply represented as  
22       “Tripleclouds”: clear, thin cloud, and thick cloud (Shonk and Hogan, 2008). Other studies have  
23       used a probability density function (PDF) representation of cloud optical depth (Barker, 1996;

1 Oreopoulos and Barker, 1999; Kato et al., 2005). For a Gamma distribution, Barker (1996)  
2 showed that the domain-averaged fluxes can be computed as a function of two parameters,  
3 expressing the PDF with a two-stream radiative transfer scheme. This approach is, however,  
4 limited to the simple two-stream radiative transfer algorithm, and also requires about four times  
5 more computational effort than the standard two-stream scheme (Barker, 1996). This approach  
6 also assumes that clouds will have uniform microphysical characteristics with a uniform single  
7 scattering albedo and asymmetry factor. But, perhaps as a more significant concern, the two-  
8 stream approach has substantial intrinsic radiative transfer uncertainty issues that are on the order  
9 of 10% compared to more precise radiative transfer modeling schemes (Barker et al., 2015; King  
10 and Harshvardan, 1986).

11 A commonly used method of estimating solar fluxes for horizontally inhomogeneous  
12 clouds is the independent column approximation (ICA). In this approach, the cloud field is  
13 partitioned into a number of subcolumns to account for the inhomogeneity. The ICA method  
14 applies a PPH radiative transfer model to each column, and then averages over all columns to  
15 obtain the domain mean fluxes. Cahalan et al. (1994b) demonstrated that the ICA fluxes could be  
16 in excellent agreement with full 3D Monte Carlo calculations. Neu et al (2007) proposed a cloud  
17 quadrature approach dividing the cloud field into four representative independent columns based  
18 on cloud optical depth. This approach could achieve an RMS error of less than 4% in actinic  
19 fluxes but the instantaneous error could be large if the cloud heterogeneity is high, or if the solar  
20 zenith angle is large (Prather. 2015).

21 The ICA approach can be considered as an accurate radiative transfer scheme to the  
22 extent that the independent columns are a good representation for inhomogeneous cloud field.  
23 But its computation time for radiative transfer increases proportionally with the number of

1 independent cloud columns. To improve the computation efficiency, several simplified methods  
2 have been developed (e.g., Evans, 1993; Barker, 1996; Gabriel and Evans, 1996; Oreopoulos and  
3 Barker 1999; Cairns et al. 2000; Kato et al., 2005). Some of these methods (e.g., Borde and Isaka  
4 1996; Cairns et al. 2000) account for the effect of cloud inhomogeneity by rescaling the bulk  
5 cloud scattering radiative parameters. As a result, the computation of radiative fluxes for the  
6 inhomogeneous cloud cases can thus be transformed into those for an equivalent single column  
7 PPH cloud. There is also the Monte Carlo Independent Column Atmosphere (McICA) method  
8 (Pincus et al., 2003) that randomly selects a sub-column as a representative of clouds in a climate  
9 GCM grid box. This stochastic approach is computationally efficient but it requires large domain  
10 averaging to reduce the sampling error.

11 As a specific example of cloud heterogeneity treatment in a climate GCM, in the Cairns  
12 et al. (2000) Monte Carlo based parameterization, the GCM grid-box-mean homogeneous cloud  
13 radiative parameters (optical depth, single scattering albedo, and asymmetry parameter) are  
14 transformed in accord with a cloud heterogeneity parameter  $V = \exp(\delta^2)$ , where  $\delta$  is the *log*  
15 standard deviation of the cloud (microscopic and/or macroscopic) density distribution. This  
16 parameterization is used in the GISS ModelE climate GCM (Schmidt et al., 2006) utilizing the  
17 Rossow et al. (2002) ( $4^\circ \times 5^\circ$  monthly-mean) empirical determination of the Cairns et al. (2000)  
18 cloud heterogeneity parameter  $V$ , based on the ISCCP D1 cloud climatology. The GISS ModelE  
19 radiation model utilizes the Single Gauss Point (SGP) doubling/adding method as its radiative  
20 transfer solver, using a look-up table to select its input radiative parameters (Hansen et al., 1983)  
21 so as to precisely reproduce the planetary albedo for any solar zenith angle and cloud optical  
22 depth for the case of conservative scattering.

1 In this paper we present a deterministic synthesizing approach to define a radiatively  
2 equivalent PPH cloud to represent an inhomogeneous cloud field, and to thus provide for  
3 efficient and accurate computation of solar fluxes for inhomogeneous clouds. Different from  
4 previous deterministic methods, the single scattering optical properties are not required to be  
5 uniform across the cloud subcolumns, and the subregion cloud optical depth distribution can be  
6 arbitrary. This method is applicable to the utilization of sophisticated 1D radiative transfer  
7 algorithms via look-up tables, which, in a sense, serve as the reference standard for comparison.  
8 Section 2 describes this synthesizing approach in detail and its use of direct and inverse look-up  
9 tables that also take on a radiative transfer solver role. Section 3 demonstrates the utility of this  
10 methodology, displaying through comparisons with ICA results the numerical errors and biases  
11 that arise for different examples of cloud heterogeneities, with concluding remarks contained in  
12 section 4.

## 13 **2. Methodology**

14 In the ICA scheme the regional, or grid-box-mean cloud fluxes represent the summation  
15 of individual cloud fluxes computed separately over all subregions of the grid-box. For a cloud  
16 field divided into N subcolumns, the ICA method conducts plane-parallel radiative transfer  
17 calculations for each column individually and then averages the subcolumn results to obtain the  
18 grid-box regional mean. Thus for example, the ICA cloud albedo is expressed as

$$A_{ICA}(\mu_0) = \sum_{i=1}^N f_i A_i(\tau_i, \mu_0) \quad (1)$$

19 where  $\mu_0$  is the cosine of the solar zenith angle.  $f_i$ ,  $A_i$  and  $\tau_i$  are the column area fraction, the PPH  
20 albedo, and the optical depth for the  $i$ th subcolumn, respectively. The ICA transmittance and  
21 absorptance for a multiple-column inhomogeneous cloud are calculated in the same manner as  
22 defined for the albedo.

1 While the ICA approach is frequently used to model radiative transfer for inhomogeneous  
2 cloud configurations, computation time can be a significant issue if the number of subcolumns is  
3 large. Here we propose an approach that combines all of the cloud subcolumns into a radiatively  
4 equivalent single column synthetic PPH cloud (labeled hereafter as sPPH for clarity), such that  
5 the ICA fluxes can be reproduced by a single plane parallel computation. To demonstrate the  
6 basic concept of this synthesizing approach, we start with a heterogeneous cloud comprised of  
7 four columns. The optical depths for the four columns are taken to be [0.3, 3, 10, 30], and the  
8 corresponding asymmetry parameters for the particle scattering functions are taken to be,  
9 respectively, [0.86, 0.84, 0.82, 0.80]. For simplicity, and not as a requirement, we assume  
10 conservative scattering and equal area fractions for all columns. For uniform solar incidence on  
11 such a 4-column cloud, the column-mean direct transmissivity ( $T_{dir}$ ) is simply

$$T_{dir} = \frac{1}{4} \sum_{i=1}^4 e^{-\tau_i/\mu_0} \quad (2)$$

12 It then follows that the effective optical depth for a sPPH cloud having the same direct  
13 transmission  $T_{dir}$  is

$$\tau_e = -\mu_0 \log(T_{dir}) \quad (3)$$

14 This derivation of the effective optical depth has also been adopted by Prather (2015). After the  
15 effective optical depth of the sPPH cloud is determined, the next step is to determine an  
16 asymmetry factor such that the sPPH cloud albedo is equal to the ICA computation. All of these  
17 properties depend on solar zenith angle. To illustrate, for a solar zenith angle of 60°, the effective  
18 optical depth of the single column sPPH cloud is 1.19, and the ICA albedo for the entire 4-  
19 column cloud is 0.4843. Through radiative transfer iteration, the effective asymmetry factor for  
20 the sPPH cloud that would reproduce the ICA column-mean albedo, is 0.232. In this way, a

1 synthetic sPPH cloud is defined that is radiatively equivalent to the heterogeneous four-column  
2 cloud. In practice, this effective asymmetry factor for the sPPH cloud would be retrieved from a  
3 pre-calculated *inverse* look-up table.

4 For our radiative transfer solver forward calculations, the forward look-up table for the cloud  
5 albedo is tabulated for a range of incident zenith angles ( $\mu_0$ ), optical depth ( $\tau$ ), asymmetry factor  
6 ( $g$ ), and single scattering albedo ( $\varpi$ ). In this table, there are a total of  $30 \times 32 \times 21 \times 18$  grid points,  
7 representing 30 grids in  $\mu_0$  from 0.02 to 1.0, 32 in  $\tau$  from 0.05 to 210, 21 in  $g$  from -0.95 to 0.95,  
8 and 18 in  $\varpi$  from 0.0 to 1.0. Because cloud albedo and transmittance approach asymptotes as  
9  $\tau$  increases, values beyond  $\tau=210$  are considered as unchanged. Since the radiative fluxes are  
10 nonlinear functions of all four variables, the grid points are unevenly distributed. For example,  
11 half of  $\varpi$  grids are in the range of 0.9 to 1.0.

12 As a general recipe, for a cloud with  $N$  columns, the complete processes to find the effective  
13 optical properties of the equivalent sPPH cloud is to:

- 14 1) Calculate the effective optical depth for the sPPH cloud according to equation (3).
- 15 2) Obtain the effective single scattering albedo,  $\varpi_e = \sum_{i=1}^N f_i \tau_i \omega_i / \sum_{i=1}^N f_i \tau_i$
- 16 3) Obtain the albedo,  $A_i(\mu_0, \tau_i, \omega_i, g_i)$ , of each column using the forward look-up-table.
- 17 4) Calculate the ICA albedo,  $A_{ICA}$ , using equation (1).
- 18 5) Find the effective asymmetry factor,  $g_e$ , corresponding to the ICA column-mean albedo,  
19 using the inverse look-up-table tabulated as a function of albedo,  $\mu_0, \tau_e$ , and  $\varpi_e$ .

20 Through this process of these five steps, a radiatively equivalent sPPH cloud to the  $N$   
21 columns of inhomogeneous cloud is found, as defined by the effective sPPH cloud optical  
22 properties  $\tau_e$ ,  $g_e$  and  $\varpi_e$ .

1 We now apply this procedure to obtain the effective sPPH optical properties for the  
2 example of the 4-column cloud described above. Figure 1 compares the albedo and transmission  
3 of the synthetic sPPH cloud with those for reference rPPH ICA results for different incident  
4 angles (the upper panel). To avoid the algorithm errors inherent in 2-stream radiative transfer  
5 schemes (Barker et al., 2015; Jin et al., 2019), we use a 16-stream discrete ordinate algorithm for  
6 all (rPPH cloud) radiative transfer and look-up table calculations. The black asterisks represent  
7 the rPPH ICA results and the red diamonds represent the results calculated from the sPPH cloud.  
8 The albedo and transmission calculated based on the simple mean cloud optical depth and mean  
9 asymmetry factor (weighted by subcolumn optical depth) are also plotted for comparison (the  
10 blue pluses). The lower panel shows the corresponding effective optical depth (black) and the  
11 asymmetry factor (red) derived for the synthetic sPPH cloud.

12 Figure 1 shows that both the ICA albedo and transmission are reproduced accurately by  
13 the simple one column of sPPH cloud. The RMS errors are only 0.25% and 0.24% for the albedo  
14 and transmission, respectively, and are due to imperfect look-up-table interpolation. However,  
15 for this specific example, the radiative transfer computation time using the synthetic sPPH cloud  
16 is reduced by a factor of 4 compared with the full ICA approach. In general, the computation  
17 time to be saved depends on the total number of cloud subcolumns. The more subcolumns, the  
18 more time is saved. Computations that simply utilize the grid-box-mean cloud optical properties  
19 might be equally as efficient in computing time, but as shown in figure 1, doing so would result  
20 in a major loss of accuracy by greatly overestimating the albedo and underestimating the  
21 transmission, compared to the synthetic sPPH approach.

22 It should be noted that the Henyey-Greenstein single scattering phase function is equally  
23 well-defined for both positive and negative values of the asymmetry parameter. Accordingly, the

1 effective asymmetry factor for the synthetic sPPH cloud can be negative because the asymmetry  
2 factor is used here as a radiative parameter that simply regulates the relative amount upward and  
3 downward scattering, and is not used, or intended, as a physical representation of real cloud  
4 properties, for which negative values of asymmetry factor are not typically encountered in  
5 nature. Thus for example, the effective asymmetry factor needed to reproduce the ICA albedo is  
6 -0.567 when  $\mu_0=0.1$  in figure 1.

7 **3. Application to General Heterogeneous Clouds**

8 Inhomogeneity in cloud distribution is often described in terms of cloud optical depth  $\tau$ .  
9 Cloud heterogeneity can be in various formats, as there is no single formula to define all possible  
10 distributions. However, previous studies have shown that the  $\tau$  distribution in many cloud fields  
11 can often be approximated by means of a Gamma distribution (e.g., Barker, 1996; Morrison and  
12 Gettelman, 2008; Oreopoulos and Barker, 1999; Oreopoulos and Cahalan, 2005; Zhang et al.,  
13 2019). The Gamma distribution function is expressed as

$$14 \quad p(\tau) = \frac{1}{\beta \Gamma(v)} \left( \frac{\tau}{\beta} \right)^{v-1} e^{-\tau/\beta} = \frac{1}{\Gamma(v)} \left( \frac{v}{\tau_m} \right)^v \tau^{v-1} e^{-v\tau/\tau_m} \quad (4)$$

15 where  $\tau_m$  is the average cloud optical depth, and  $v$  is the gamma distribution shape parameter.  
16  $\Gamma(v)$  is the Gamma function and  $v = (\tau_m/\sigma)^2$  in which  $\sigma$  is the standard deviation of  $\tau$ . Smaller  
17  $v$  indicates a higher degree of inhomogeneity.  $\beta = \tau_m/v$  is the scale parameter. The larger the  
18 scale parameter, the more spread out the distribution.

19 Figure 2 shows an example of the Gamma distribution with mean optical depth  $\tau_m=10$   
20 for four different shape parameters ( $v$ ), in which  $v=8$  represents the least heterogeneity, and  
21  $v=0.5$  represents the most heterogeneous case. The horizontal axis depicts the cloud optical depth  
22  $\tau$  in logarithmic scale. Different bars represent the probability or cloud fraction in a different  $\tau$

1 bin. The bin width is uniformly 0.5 in logarithmic scale. Each bin center corresponds to the mean  
2  $\tau$  of the bin, which is 0.05 for the left-most bin, and 148 for the right-most bin in Figure 2. As  
3  $v$  decreases, the distribution range of  $\tau$  increases. A broad range of cloud inhomogeneities can be  
4 approximated by different combinations of  $v$  and  $\tau_m$  in the distribution function of Equation (4).

5 We now apply the synthetic approach to inhomogeneous clouds with four different shape  
6 parameters as shown in figure 2, and with different mean optical depth  $\tau_m$ . Each bin in figure 2  
7 is considered as one cloud subcolumn, and the probability for each bin is the cloud fraction for  
8 the subcolumn. Clearly, the cloud field with smaller  $v$  will have more cloud columns because of  
9 wider variation range of  $\tau$ . In our actual calculations, we ignore those columns with PDF value  
10 (cloud fraction) less than 0.01, or  $\tau$  less than 0.28. Under these conditions, the total number of  
11 cloud columns is 4 for  $v = 8$  and 12 for  $v = 0.5$  for the example shown in figure 2. It should be  
12 noted that this synthetic method could be applied to any  $\tau$  distribution. We use the Gamma  
13 distribution here because it is convenient and representative.

14 Figure 3 shows the biases in albedo and transmission calculated with the synthetic sPPH  
15 cloud from the ICA calculations. Again, albedo and transmission for each cloud subcolumn and  
16 the rPPH cloud are calculated using the 16-stream radiative transfer scheme. The number of  
17 cloud subcolumns and the fraction of each column for ICA are generated as shown in figure 2.  
18 The horizontal and vertical coordinates in each panel represent the cosine of the solar zenith  
19 angle ( $\mu_0$ ), and the cloud mean optical depth in logarithmic scale ( $\log(\tau_m)$ ), respectively.  
20 Different rows depict a different heterogeneity parameter. The left panels show the relative  
21 biases of albedo in per cent, and the right panels show the transmission biases. Because the  
22 transmission at large optical depth or large incident angle could be near zero, where tiny  
23 differences could appear very large on a relative scale, the transmission bias is presented as

1 actual differences times a factor of 100. The dotted white lines are contours of bias. Conservative  
2 scattering and a Henyey-Greenstein cloud scattering asymmetry factor of 0.86 are assumed here.  
3 Regardless of the degree of inhomogeneity, figure 3 shows that the relative albedo biases for all  
4 incident angles are less than 0.5% and that the transmission differences are within  $\pm 0.003$ .

5 Figure 4 compares the spherical albedo and transmission between the ICA approach and  
6 the synthetic PPH approximation. The spherical albedo (transmission) can be regarded as the  
7 averaged albedo (transmission) over all incident angles. Different panels represent a different  
8 cloud inhomogeneity. In each panel, the black asterisk is for ICA calculation and the red  
9 diamond is for that of the synthetic PPH approximation. The horizontal axis represents the  
10 logarithmic cloud mean optical depth,  $\log(\tau_m)$ . Again, both the ICA albedo and transmission  
11 based on the synthetic PPH cloud agree well with the intensive ICA computations in all cases.  
12 The RMS errors in both the spherical albedo and transmission are 0.0004. Again, this small error  
13 is simply due to imperfect interpolation of look-up-table variables, which is the only error source  
14 when the scattering is conservative.

15 For conservative scattering, transmission has the same biases as the albedo but with  
16 opposite direction. However, as shown in figure 5, this does not apply for non-conservative  
17 scattering cases, in which case, a correct transmittance requires not only accurate reflection but  
18 also accurate in-cloud absorption. Figure 5 is a counterpart of figure 3 but with particle single  
19 scattering albedo of 0.98. For this absorptive case, the albedo bias is as small as in conservative  
20 scattering, but the transmission bias becomes much larger. Generally, the transmission is  
21 positively biased and the bias increases systematically with the optical depth. It also increases as  
22 the cloud inhomogeneity increases. Under non-conservative scattering conditions, scaling the  
23 single scattering albedo is required to reduce the bias. We have found that the transmission bias

1 can be significantly reduced by applying the following scaling factor to the effective single  
2 scattering albedo ( $\omega_e$ )

3

$$C = e^{-\left[\omega_e^{0.4}(1-\omega_e)^{0.8}\left(\frac{3.2}{(\tau_e+2)^{1.2}}+0.1\right)\left(3.5\left(1-\frac{\tau_e^0}{\tau_{mn}}\right)^{1.3}+0.1\right)S(6-1.5\tau_a)\right]} \quad (5)$$

4 where  $\tau_{mn}$  is the mean cloud optical depth averaged in logarithmic scale and  $\tau_e^0$  is the effective  
5 optical depth of the synthetic PPH cloud for a  $\mu_0 = 1$  solar zenith angle.  $\tau_a = \tau_e(1 - \omega_e)$  is the  
6 absorptive optical depth of the synthetic cloud.  $S$  represents the Sigmoid function, which is  
7  $S(x) = \frac{1}{1+e^{-x}}$ . For either conservative scattering ( $\omega_e=1.0$ ) or total absorption ( $\omega_e=0$ ), the  
8 synthetic approach is accurate, and thus there is no correction required. In these special cases, the  
9 scaling factor  $C$  from equation (5) is 1.0, indicating no adjustment applied to  $\omega_e$ . As  $\tau_a$  increases,  
10 the Sigmoid function rapidly approaches zero, in which case, no adjustment is required either.

11 Figure 6 shows the same computation as figure 5, but with the adjustment of equation (5)  
12 applied to the effective single scattering albedo of the sPPH cloud. In comparing figure 6 to  
13 figure 5, the bias in albedo is found to be similar without much effect, but the bias in  
14 transmission is reduced significantly.

15 Figure 7 compares the spherical albedos and transmissions for this absorptive condition  
16 ( $\omega_e=0.98$ ) with different panels representing a different inhomogeneity. In each panel, the black  
17 line is for rPPH ICA calculations, the blue is for the synthetic sPPH approach without adjustment  
18 of  $\omega_e$ , and the red with adjustment of  $\omega_e$ . The results show that the transmission can be well  
19 simulated after the  $\omega_e$  adjustment except for the highly heterogenous clouds with large mean  
20 optical thickness, while the albedo is accurately simulated regardless of the adjustment.

21 The computations thus presented have demonstrated the methodology of the synthetic  
22 sPPH approach but have used the artificially assumed cloud optical properties and uniform

1 microphysical cloud characteristics. In more realistic situations, not only the optical depth, but  
2 the single scattering albedo and the asymmetry factor can also be arbitrarily distributed within  
3 the different subcolumns. This can be readily handled using the synthetic sPPH method.

4 We now perform further tests of the algorithm using the optical properties based on real  
5 cloud particle size and phase. The particle size is allowed to vary randomly in different columns.  
6 The variation range of the effective cloud particle radius is from 7  $\mu\text{m}$  to 80  $\mu\text{m}$ . The cloud  
7 composition is considered to be water if the radius is less than 17  $\mu\text{m}$ , otherwise it is treated as  
8 ice. For ice cloud optical properties, we use the surface-roughened aggregate model used in the  
9 MODIS Collection 6 cloud product (Platnick et al., 2017). For liquid cloud, the spherical water  
10 particle model developed by Hu and Stamnes (1993) is used. The same heterogeneous cloud  
11 fields as were used for Figures 3-7 are used to calculate the broadband shortwave fluxes and to  
12 evaluate biases in the calculated solar radiation. The incident solar spectrum is taken from  
13 MODTRAN 1  $\text{cm}^{-1}$  resolution data (Berk et al., 2008). Spectral integrals are performed over the  
14 0.3 to 5.0  $\mu\text{m}$  range, but without including Rayleigh scattering, aerosols, or gaseous absorbers.

15 Figure 8 is the counterpart of figure 6 but shows the biases in shortwave albedo and  
16 transmission for inhomogeneous clouds with nonuniform microphysical properties. Figure 9  
17 compares the spherical (or all-angle averaged) albedo and transmission calculated from the  
18 synthetic sPPH cloud, along with those from the reference rPPH ICA computation. The results in  
19 figure 8 indicate that the biases are within  $\pm 0.7\%$  for the broadband shortwave albedo and  
20  $\pm 0.015$  in transmission for all incident angles and heterogeneity cases. The relative RMS biases  
21 for the spherical albedo and transmission are 0.26% and 0.76%, respectively.

22 If the water and ice clouds are not mixed between different columns, the biases are even  
23 smaller than those shown in figures 8 and 9. We show in Figures 10 and 11 only the spherical

1 shortwave albedo and transmission for water cloud and ice cloud, respectively. In these  
2 calculations, the effective particle radius was allowed to change randomly in the 17 to 80  $\mu\text{m}$   
3 range for ice cloud, and in the range of 7 to 17  $\mu\text{m}$  for water cloud columns. The relative RMS  
4 biases for the spherical albedo and transmission of water clouds are 0.24% and 0.48%,  
5 respectively. Similarly, the RMS biases of albedo and transmission for ice clouds are 0.25% and  
6 0.52%, respectively. In comparing figures 10 and 11 with figure 9, not only are the biases  
7 smaller, but the albedo and transmission lines, representing their variation with the mean cloud  
8 optical depth, are also smoother. This is because there is only one cloud phase and thus a smaller  
9 variation in the optical properties among different columns. In comparing figure 10 with figure  
10 11, we see that the water cloud has a higher albedo and a lower transmission than the ice cloud  
11 for the same optical depth for all heterogeneous cases.

12 Table 1 summarizes the RMS biases of the synthetic PPH method in the spherical  
13 shortwave albedo and transmission for the different cloud inhomogeneities and particle size  
14 ranges. The numbers in parenthesis represent the relative biases in per cent. The bias in spherical  
15 albedo is generally small (less than 0.4%) regardless of the cloud heterogeneity and particle size  
16 variation. The bias in transmission is larger but still less than 1%, and in most cases, tends to  
17 show somewhat of an increase as the variation range of the cloud particle size increases.

18 We have found that occasionally the ICA albedo can become so high that the effective  
19 asymmetry factor interpolated from the inverse look-up table approaches the bounds of the table.  
20 This usually occurs for extreme near-horizontal incidence conditions (cosine of solar zenith  
21 angle less than 0.1) for some non-conservative scattering cases. When this happens, we decrease  
22 the effective single scattering co-albedo ( $1-\omega_e$ ) by 10%, which increases  $\omega_e$  by the amount of  
23  $0.1(1-\omega_e)$ . We then go back to the look-up table to find the new effective asymmetry factor.

1     **5. Discussion and Conclusions**

2           We describe a new method for computing the mean radiative fluxes for inhomogeneous  
3        cloud fields. A radiatively equivalent sPPH cloud can be found to represent the multiple column  
4        horizontally inhomogeneous cloud, being transformed into the more tractable plane parallel  
5        cloud framework. In ICA, a horizontally inhomogeneous cloud region is divided into a number  
6        of subregions and radiative transfer computation is applied to each subregion individually. Using  
7        the synthetic sPPH cloud, the radiative transfer computation for all subcolumns is transformed  
8        into a single column regardless of the total number of subcolumns that may be used initially to  
9        represent the cloud inhomogeneity. The effective optical depth of the synthetic sPPH cloud is  
10       derived by matching the direct transmission to that of the inhomogeneous cloud field, which is  
11       calculated as the subcolumn average in ICA. The effective scattering asymmetry factor, which is  
12       allowed to vary from -1.0 to 1.0, is found from a pre-calculated inverse albedo look-up-table.

13       We examined the biases of the synthetic sPPH method by comparing to the rPPH results  
14       from ICA. For the special cases of conservative scattering (or total absorption), the synthetic  
15       method is exact, and the radiative fluxes calculated would be equal to the ICA results, with the  
16       small biases (about 0.2%) in the sPPH cases arising entirely due to imperfect interpolation in  
17       using the forward look-up table. In principle, since this is primarily a function of the look-up  
18       tables, the ICA albedo can be accurately approximated by the sinlge column synthetic sPPH  
19       cloud, regardless of cloud inhomogeneity. However, to obtain accurate transmission in  
20       absorptive cases, a scaling factor is required to adjust the effective single scattering albedo. We  
21       have tested the synthetic sPPH approach on cloud fields with different inhomogeneities and a  
22       wide range of cloud particle properties. The broadband shortwave albedo and transmission agree  
23       well with the corresponding rPPH ICA computations. Averaged over all incident directions, the

1 shortwave albedo and transmission calculated from the synthetic sPPH cloud have RMS errors of  
2 0.26% and 0.76%, respectively, for inhomogeneous clouds over a wide range of particle size  
3 with ( $R_e$ ) ranging from 7 to 80  $\mu\text{m}$ . The accuracy would be even higher for narrower cloud  
4 microphysical property variation.

5 Compared with many approximate methods for modeling cloud inhomogeneities, the  
6 advantages of the synthetic sPPH method developed here are that (1) it is not required that all the  
7 cloud subcolumns have uniform microphysical characteristic (i.e., the same single scattering  
8 albedo and scattering asymmetry factor), (2) it can be applied to sophisticated radiative transfer  
9 schemes, (3) it can handle arbitrary cloud optical depth distributions and an arbitrary number of  
10 subcolumns, and (4) it is straightforward to implement.

11 Although the synthetic sPPH method is computationally efficient and accurate, there are  
12 some limitations. The computation accuracy of this method has been evaluated against the rPPH  
13 ICA calculations and its viability rests on the assumption that the ICA approach is a reliable  
14 reference point. Therefore, potential 3D radiative interactions between the different cloud  
15 subcolumns is not included in the computations presented. Furthermore, the sPPH approach has  
16 currently been applied only to single layer cloud cases. Future work should consider cloud  
17 overlapping and its effect on atmospheric heating rate.

18

19 **Acknowledgement:**

20 This study is supported by the NASA Modeling, Analysis, and Prediction (MAP)  
21 program (grant NNH10ZDA001N). Z. Jin acknowledges support from the NASA's  
22 Interdisciplinary Research in Earth Science (IDS) program (award 19-IDS19-0059).

## References

- Barker, H. W. (1996), A parameterization for computing grid-averaged solar fluxes for inhomogeneous marine boundary layer clouds: 1. Methodology and homogeneous biases, *J. Atmos. Sci.*, 53(16), 2289–2303.
- Barker, H. W., J. N. S. Cole, J. Li, B. Yi, and P. Yang, 2015: Estimation of errors in two-stream approximations of the solar radiative transfer equation for cloudy-sky conditions. *J. Atmos. Sci.*, 72, 4053–4074, <https://doi.org/10.1175/JAS-D-15-0033.1>.
- Bäuml, G., A. Chlond, E. Roeckner, Estimating the PPH-bias for simulations of convective and stratiform clouds, *Atmospheric Research*, 72, 317-328, 2004.
- Berk, A., G.P. Anderson, P.K. Acharya, and E.P. Shettle, 2008: MODTRAN5 Version 2 USERS MANUAL, SPECTRAL SCIENCES, INC, Burlington MA and Air force Geophysics Laboratory, Hanscom AFB, MA.
- Bomidi Lakshmi Madhavan, John Kalisch, and Andreas Macke, Shortwave surface radiation network for observing small-scalecloud inhomogeneity fields, *Atmos. Meas. Tech.*, 9, 1153–1166, 2016.
- Borde, R., and H. Isaka, 1996: Radiative transfer in multifractal clouds. *J. Geophys. Res.*, 101, 29 461–29 478.
- Cahalan, R. F., W. Ridgway, W. J. Wiscombe, T. L. Bell, and J. B. Snider (1994a), The albedo of fractal stratocumulus clouds, *J. Atmos. Sci.*, 51(16), 2434–2455.
- Cahalan, R. T., W. Ridgway, W. J. Wiscombe, S. Gollmer, and Harshvardhan, 1994b: Independent pixel and Monte Carlo estimate of stratocumulus albedo. *J. Atmos. Sci.*, 51, 3776–3790.

- Cairns, B., A. A. Lacie, and B. E. Carlson, 2000: Absorption within inhomogeneous clouds and its parameterization in general circulation models. *J. Atmos. Sci.*, 57, 700–714.
- Carlin, B., Q. Fu, U. Lohmann, G. G. Mace, K. Sassen, and J. M. Comstock, 2002: High-cloud horizontal inhomogeneity and solar albedo bias. *J. Climate*, 15, 2321–2339.
- Gabriel, P. M., and K. F. Evans, 1996: Simple radiative transfer methods for calculating domain-averaged solar fluxes in inhomogeneous clouds. *J. Atmos. Sci.*, 53, 858–877.
- Hansen, J.E. and L.D. Travis, 1974: Light scattering in planetary atmospheres. *Space Sci. Rev.* 16, 527–610, doi:10.1007/BF00168069.
- Hansen, J., G. Russell, D. Rind, P. Stone, A. Lacis, S. Lebedeff, et al., 1983: Efficient three-dimensional global models for climate studies: Models I and II. *Mon. Weather Rev.*, 111, 609–662.
- Hogan, R. J., S. A. K. Schäfer, C. Klinger, J.-C. Chiu and B. Mayer, 2016: Representing 3D cloud-radiation effects in two-stream schemes: 2. Matrix formulation and broadband evaluation. *J. Geophys. Res.*, 121, 8583–8599.
- Hu, Y. X., and K. Stamnes, 1993: An accurate parameterization of the radiative properties of water clouds suitable for use in climate models. *J. Climate*, 6, 728–742.
- Jin, Z., Y.-C. Zhang, A. Del Genio, G. Schmidt, and M. Kelley, 2019: Cloud scattering impact on thermal radiative transfer and global longwave radiation. *J. Quant. Spectrosc. Radiat. Transfer*, 239, 106669, doi:10.1016/j.jqsrt.2019.106669.
- Kato, S., F. G. Rose, T. P. Charlock, Computation of domain-averaged irradiance using satellite-derived cloud properties, *J. Atmos. Meas. Oce. Tech.*, 22, 146–164., 2005.
- King, M. D., and Harshvardhan, 1986: Comparative accuracy of selected multiple scattering approximations. *J. Atmos. Sci.*, 43, 784–801.

- King, M. D., S. Platnick, W. P. Menzel, S. A. Ackerman, and P. A. Hubanks, 2013: Spatial and temporal distribution of clouds observed by MODIS onboard the Terra and Aqua satellites. *IEEE Trans. Geosci. Remote Sens.*, 51, 3826–3852.
- Morrison, H. and A. Gettelman, 2008: A new two-moment bulk stratiform cloud microphysics scheme in the Community Atmosphere Model, version 3 (CAM3). Part I: Description and numerical tests, *J. Climate*, <https://doi.org/10.1175/2008JCLI2105.1>.
- Neu, J. L., Prather, M. J., and Penner, J. E., 2007: Global atmospheric chemistry: Integrating over fractional cloud cover, *J. Geophys. Res.-Atmos.*, 112, D11306.
- Oreopoulos, L., and H. W. Barker, 1999: Accounting for subgrid-scale cloud variability in a multi-layer 1D solar radiative transfer algorithm. *Quart. J. Roy. Meteor. Soc.*, 125, 301–330.
- Oreopoulos, L., and R. Cahalan, 2005: Cloud Inhomogeneity from MODIS. *J. Climate*, 18 (23): 5110–5124.
- Pincus, R., H. W. Barker, and J.-J. Morcrette, 2003: A fast, flexible, approximate technique for computing radiative transfer in inhomogeneous clouds. *J. Geophys. Res. Atmos.*, 108, 4376, doi:10.1029/2002JD003322.
- Platnick, S., and Coauthors, 2017: The MODIS cloud optical and microphysical products: Collection 6 updates and examples from Terra and Aqua. *IEEE Trans. Geosci. Remote Sens.*, 55, 502–525, <https://doi.org/10.1109/TGRS.2016.2610522>.
- Prather, M. J.: Photolysis rates in correlated overlapping cloud fields: Cloud-J 7.3c, *Geosci. Model Dev.*, 8, 2587–2595, <https://doi.org/10.5194/gmd-8-2587-2015>, 2015.
- Rossow, W. B., C. Delo, and B. Cairns, 2002: Implications of the observed mesoscale variations of clouds for the Earth's radiation budget. *J. Climate*, 15, 557–585.

- Schmidt, G.A., R. Ruedy, J.E. Hansen, I. Aleinov, N. Bell, M. Bauer, et al., 2006: Present day atmospheric simulations using GISS ModelE: Comparison to in-situ, satellite and reanalysis data. *J. Climate*, 19, 153–192, doi:10.1175/JCLI3612.1.
- Shonk, J. K. P., and R. J. Hogan, 2008: Tripleclouds: an efficient method for representing horizontal cloud inhomogeneity in 1D radiation schemes by using three regions at each height. *J. Climate*, 21, 2352–2370.
- Zhang Z., H. Song, P.-L. Ma, V. E. Larson, M. Wang, X. Dong, and J. Wang, Subgrid variations of the cloud water and droplet number concentration over the tropical ocean: satellite observations and implications for warm rain simulations in climate models, *Atmos. Chem. Phys.*, 19, 1077–1096, 2019.

**Table 1. RMS Errors in Spherical Albedo and Transmission**

Cloud Type ( $R_e$ range)	RMS Albedo Error				RMS Transmission Error			
	v=8.0	v=4.0	v=1.0	v=0.5	v=8.0	v=4.0	v=1.0	v=0.5
Water (7-17 $\mu\text{m}$ )	0.0004 (0.10)	0.0008 (0.23)	0.0010 (0.30)	0.0010 (0.32)	0.0015 (0.25)	0.0020 (0.34)	0.0041 (0.65)	0.0034 (0.52)
Ice (17-80 $\mu\text{m}$ )	0.0011 (0.25)	0.0011 (0.26)	0.0008 (0.22)	0.0010 (0.27)	0.0028 (0.55)	0.0026 (0.51)	0.0027 (0.50)	0.0030 (0.53)
Mixed (7-80 $\mu\text{m}$ )	0.0011 (0.26)	0.0011 (0.26)	0.0008 (0.21)	0.0010 (0.28)	0.0046 (0.89)	0.0033 (0.65)	0.0034 (0.62)	0.0048 (0.83)

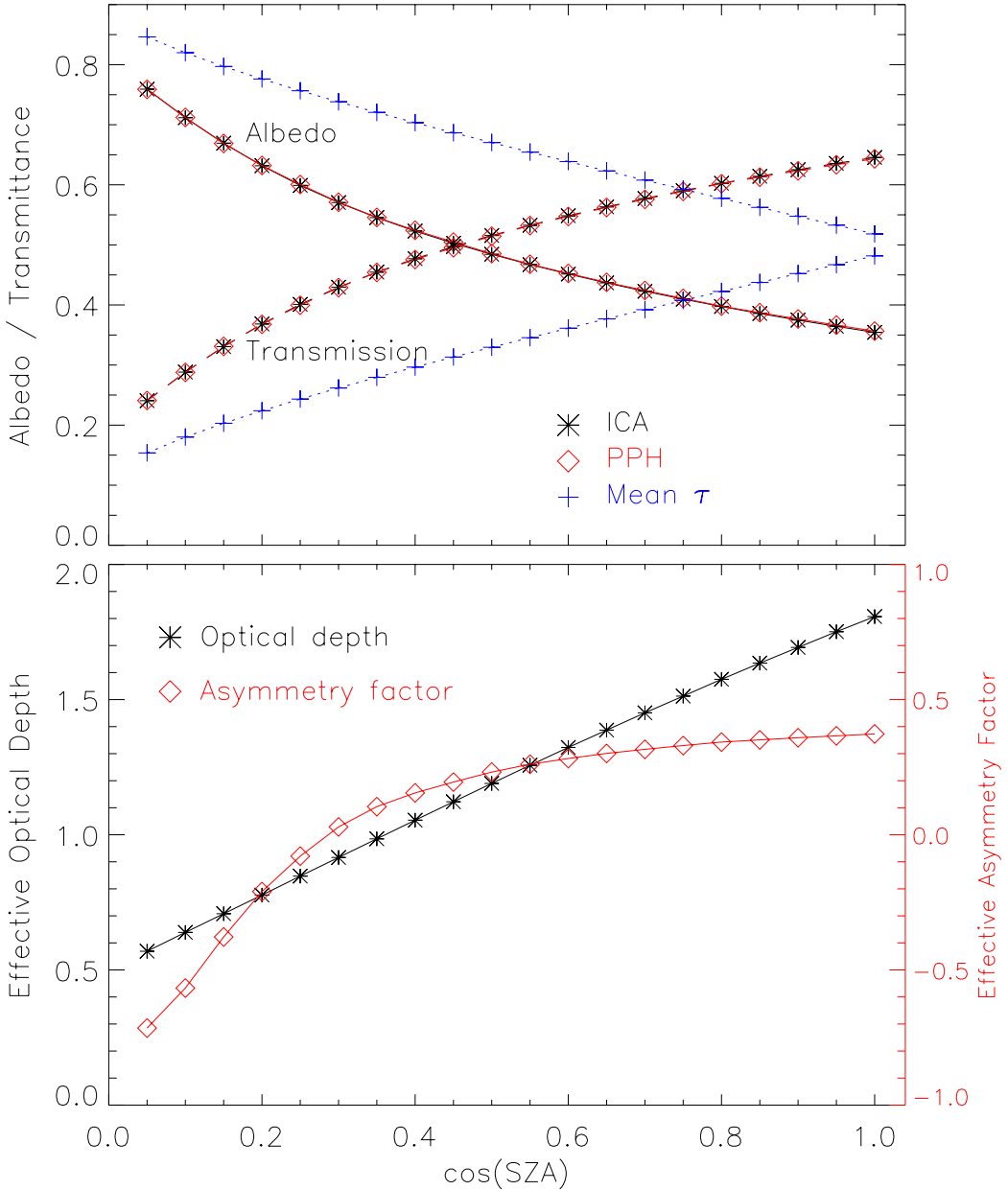


Fig. 1. Upper panel compares the albedo and transmittance of a 4-column cloud (see text for description) between the ICA method (black) and the synthetic PPH approach (red). The blue pluses represent the albedo and transmission calculated based on the simple mean cloud optical properties. Lower panel shows the corresponding effective optical depth and scattering asymmetry factor for the synthetic PPH cloud.

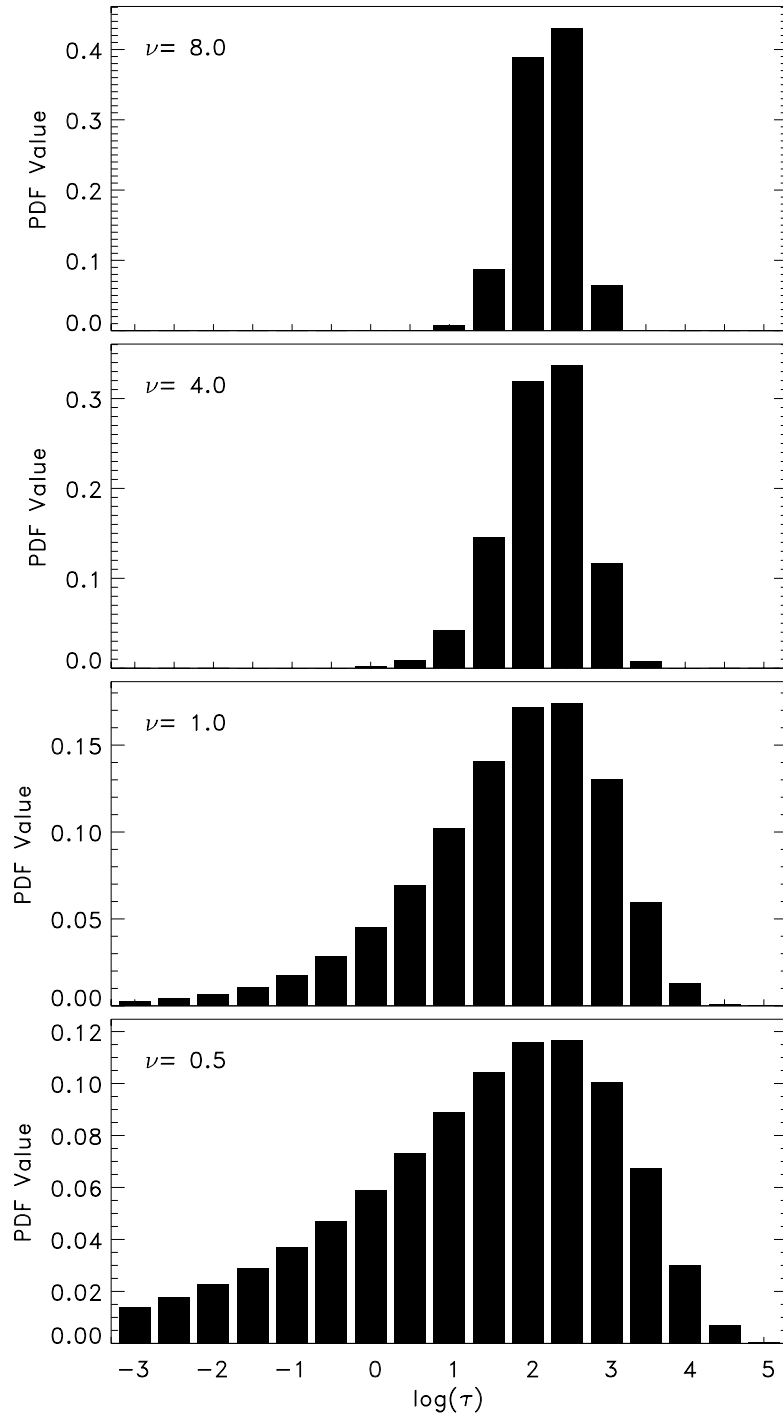
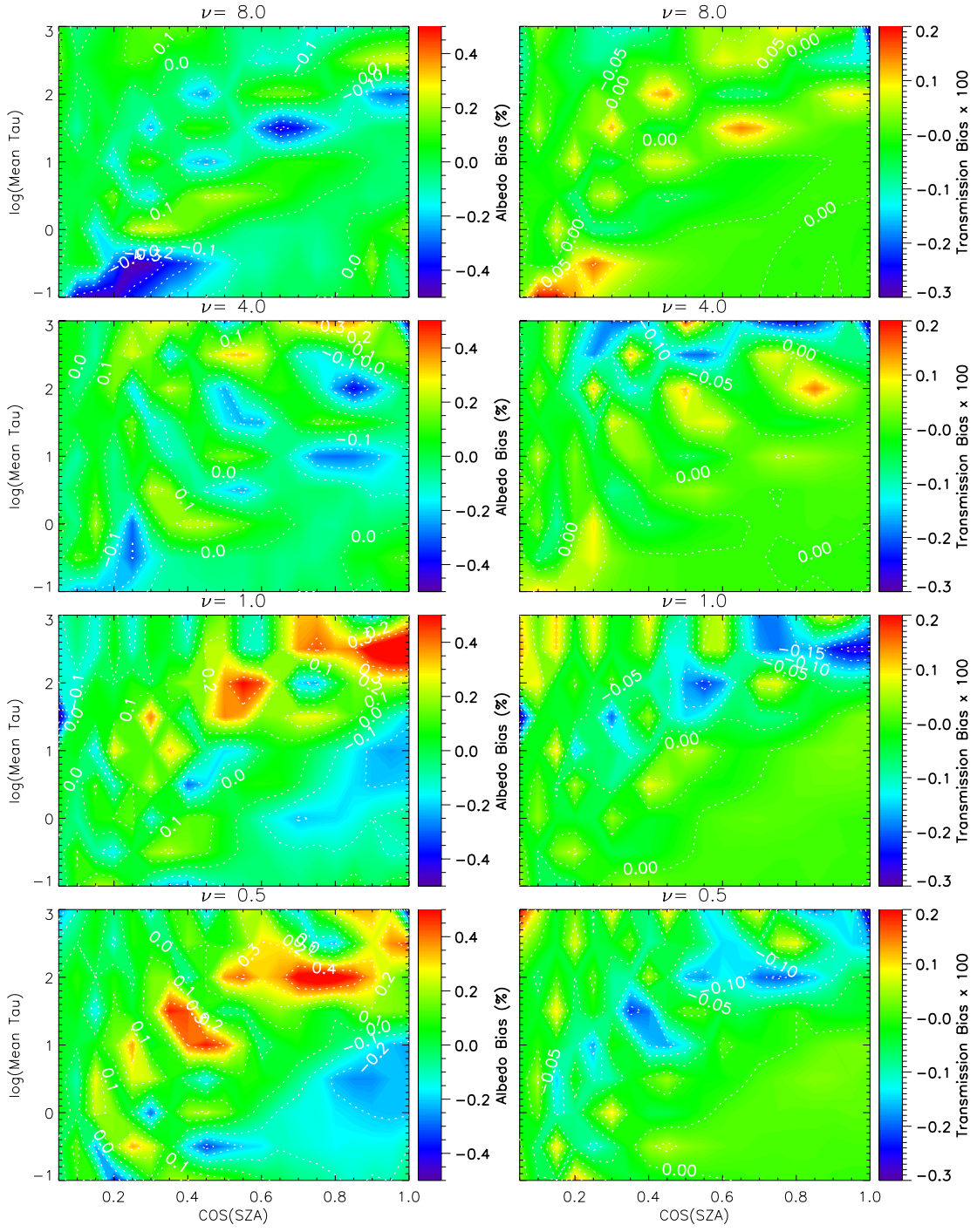


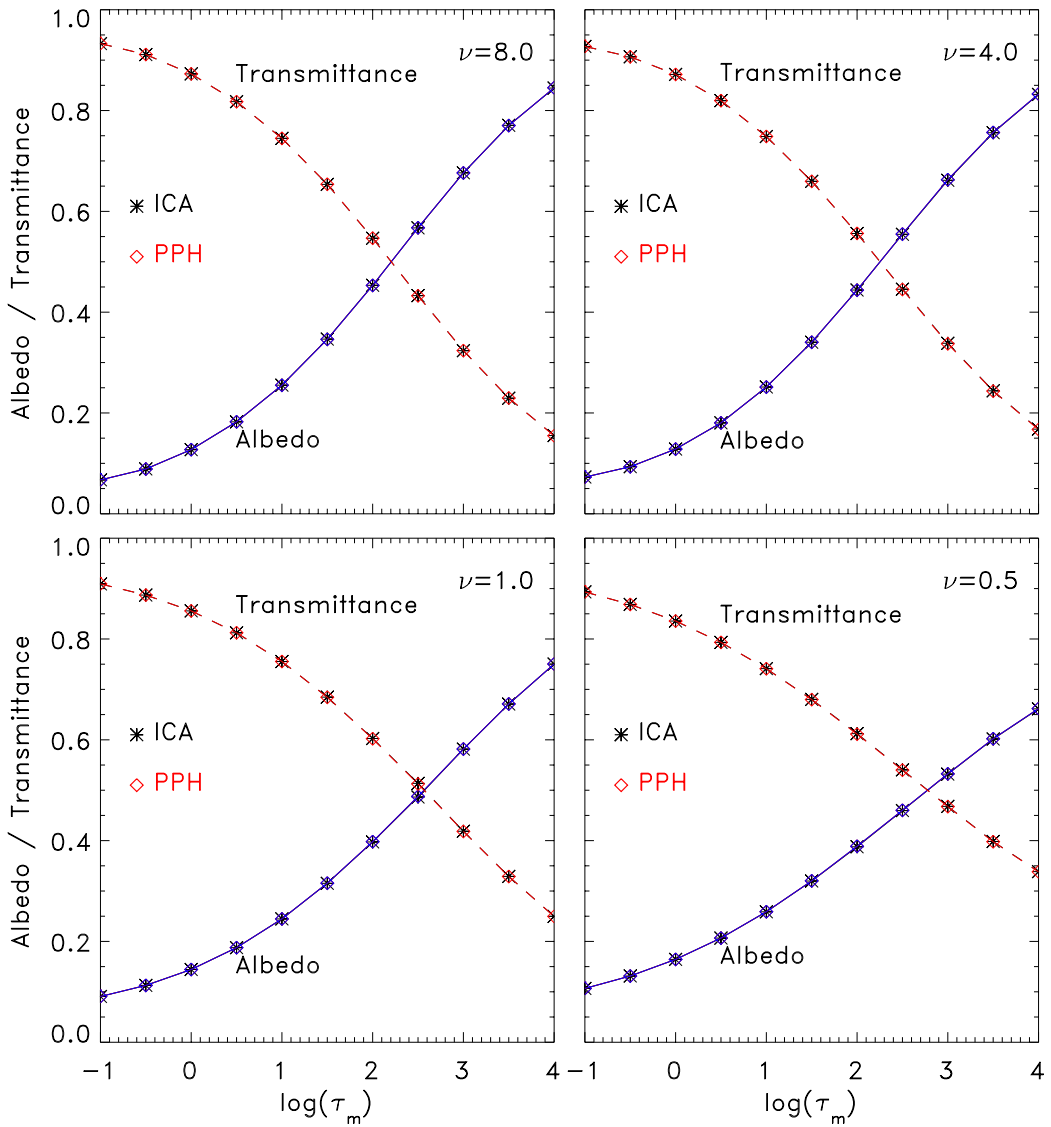
Fig. 2. An example of Gamma distributions with mean optical depth  $\tau_m=10$  for four different shape parameters,  $\nu$ . Heterogeneity increases from top ( $\nu=8$ ) to bottom ( $\nu=0.5$ ). A different bar represents the probability or cloud fraction in a different  $\log(\tau)$  bin of 0.5 in width.



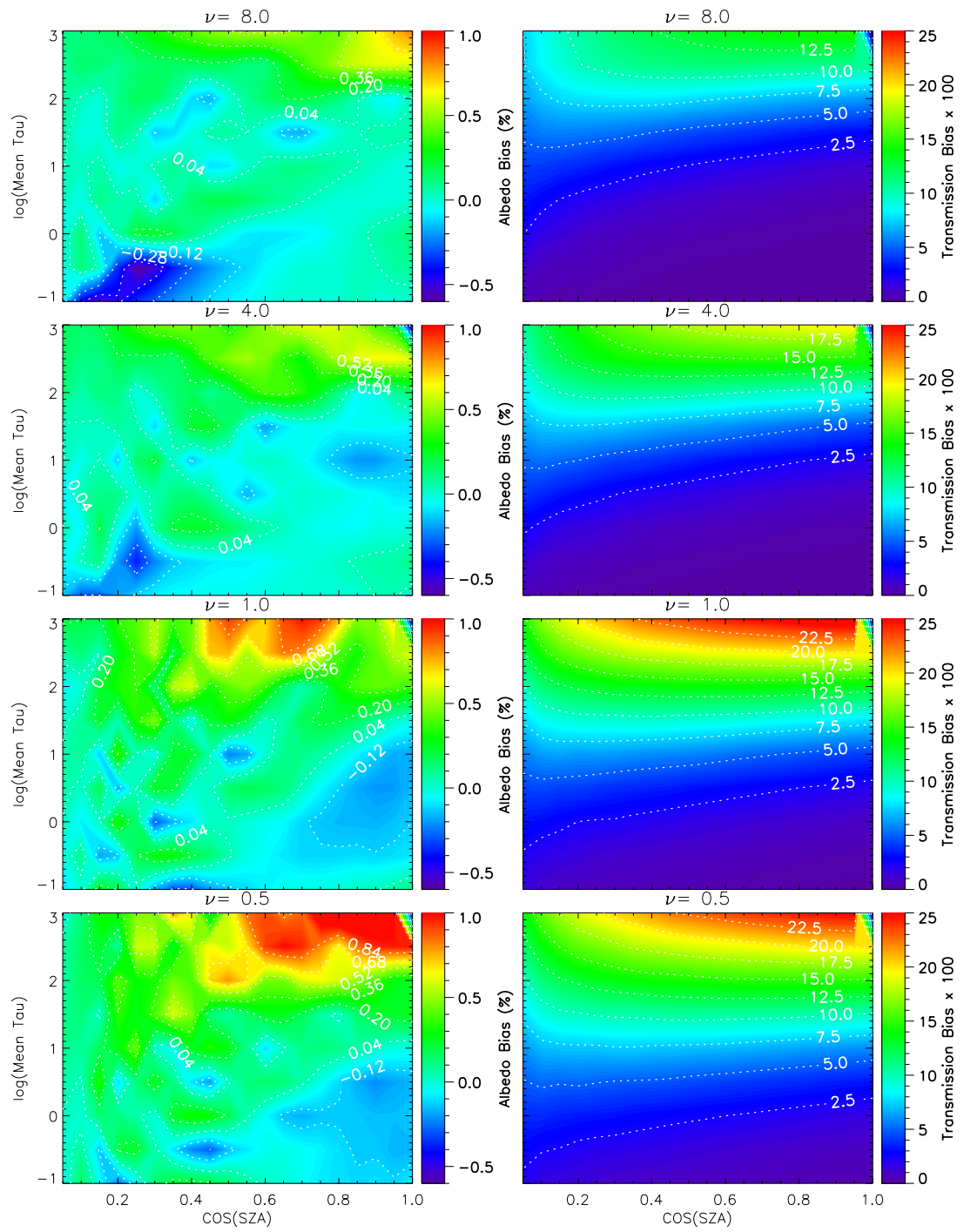
1

Fig. 3. Biases in albedo (left) and transmission (right) calculated with the synthetic PPH cloud from the ICA calculations. The horizontal and vertical coordinates in each panel represent the cosine of zenith angle and the cloud mean optical depth ( $\log(\tau_m)$ ), respectively. The number of cloud subcolumns and the fraction of each column are generated as in figure 2.

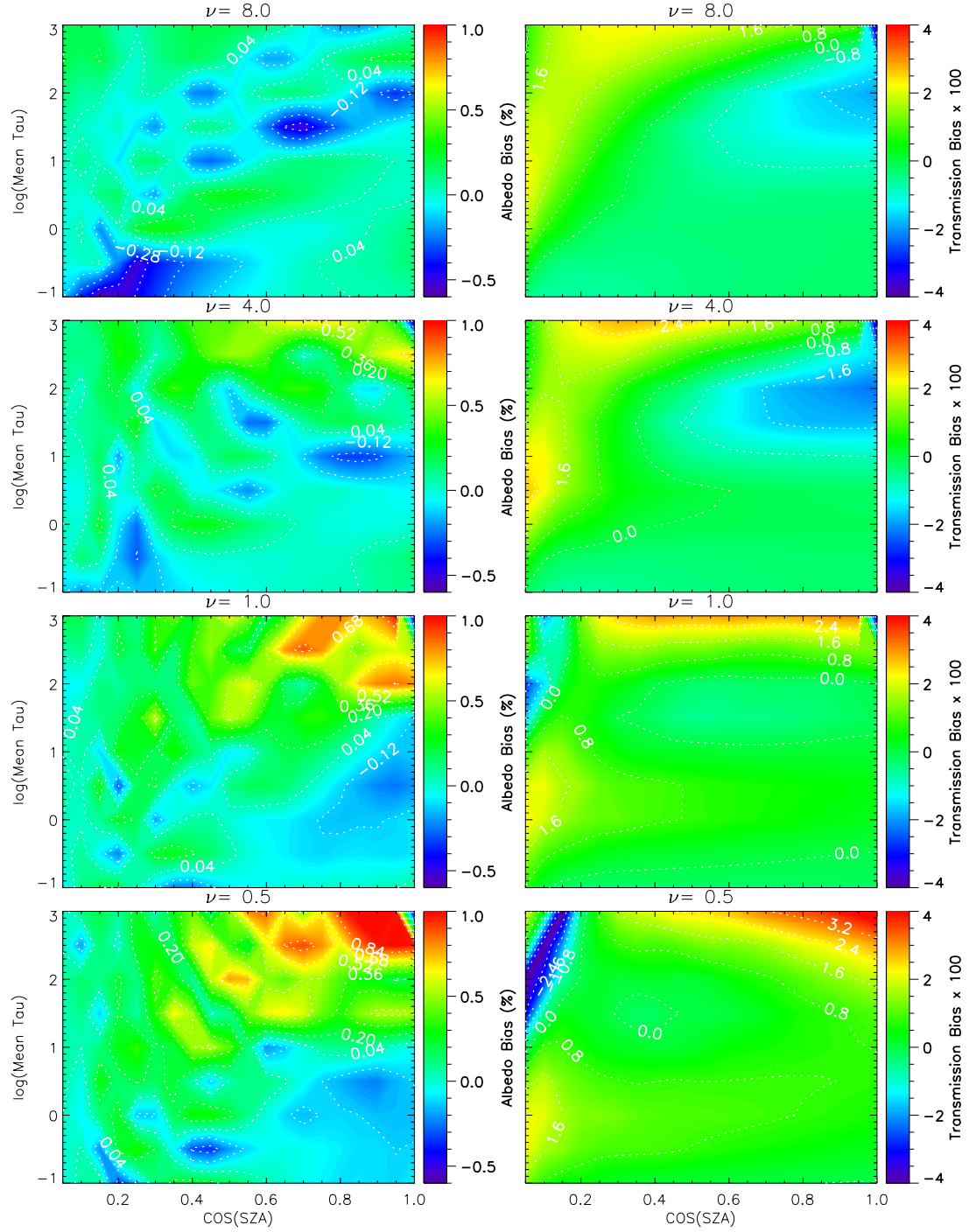
2



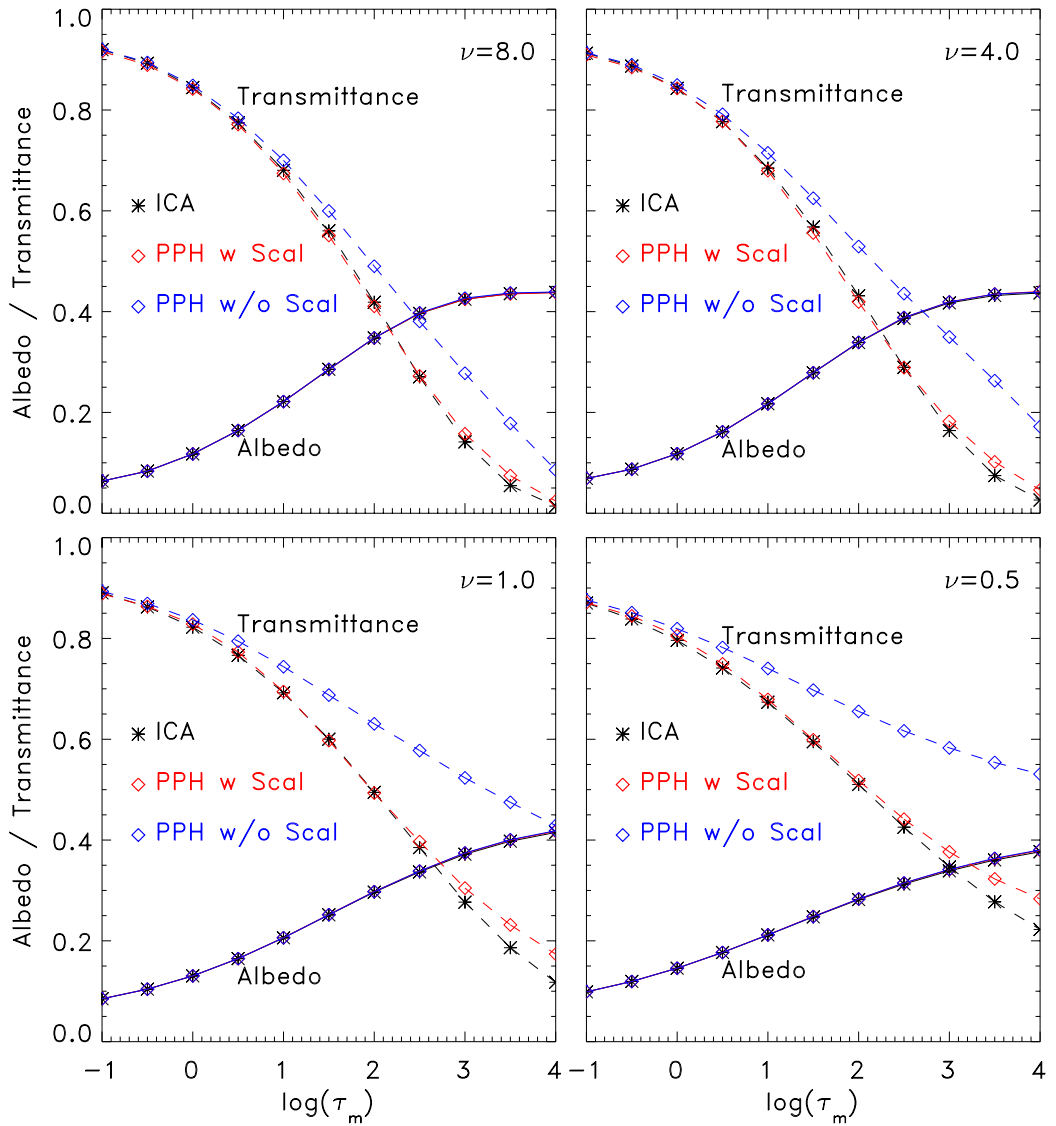
1 Fig. 4. Comparison of spherical albedo and transmission between the ICA approach (black) and  
2 the synthetic PPH approximation (red). A different panel represents a different cloud  
inhomogeneity.  $\tau_m$  is the mean cloud optical depth.



1 Fig. 5. As in Figure 3 except this is for a nonconservative scattering  
2 with single scattering albedo of 0.98.



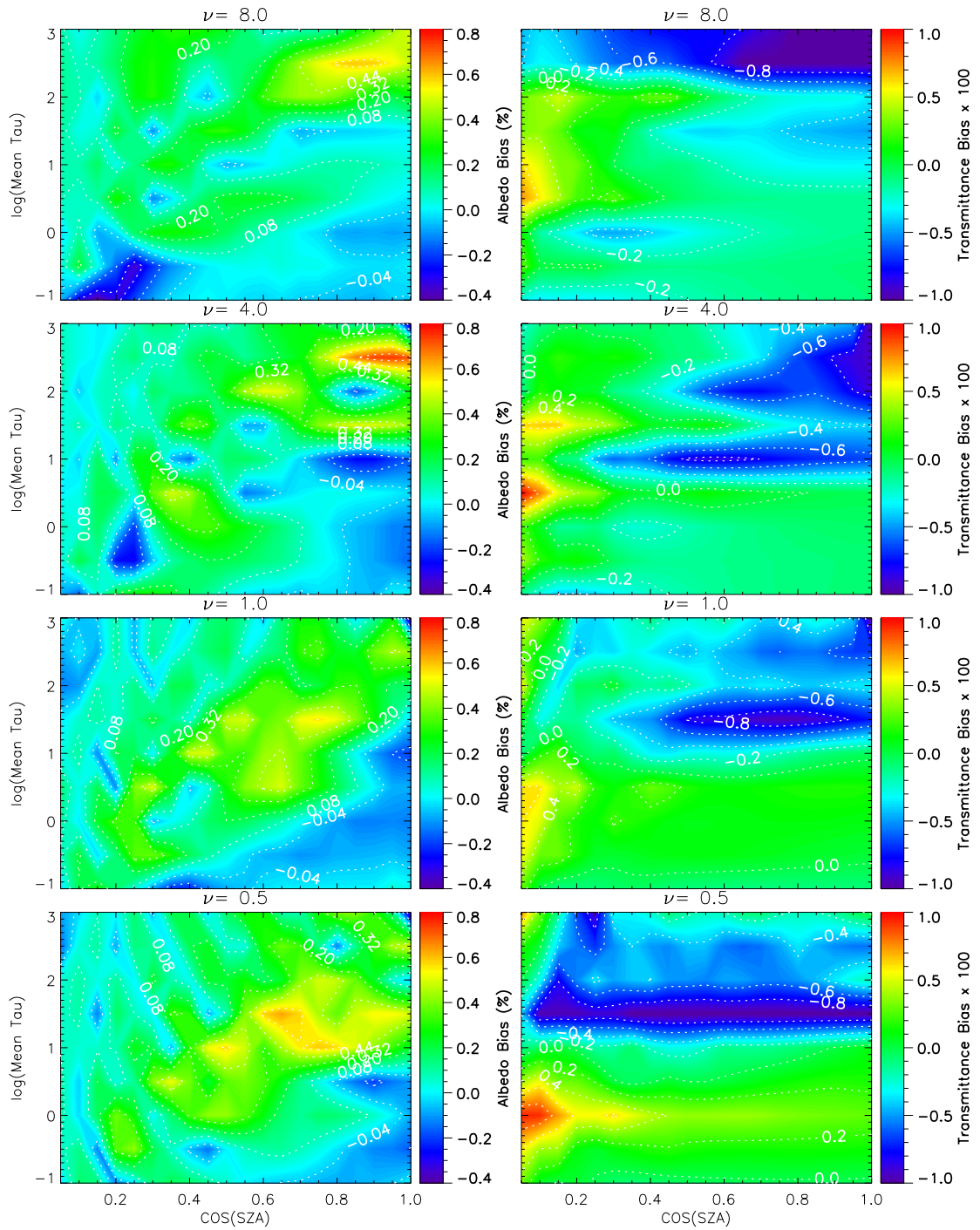
1 Fig. 6. As in Figure 5 except an adjustment of the effective single scattering albedo as in  
2 Equation (5) is applied to the PPH cloud.



1

Fig. 7. Comparison of spherical albedo and transmission between the ICA approach (black), the synthetic PPH approximation (blue), and the synthetic PPH with scaling of the single scattering albedo (red). Cloud single scattering albedo is 0.98.

2



1

Fig. 8. As in Figure 6 but these are for solar radiation calculated with real could optical properties. The cloud particle effective radius is allowed to vary randomly from  $7 \mu\text{m}$  to  $80 \mu\text{m}$  among cloud subcolumns. Particle size less than  $17 \mu\text{m}$  is assumed as water and as ice otherwise.

2

3

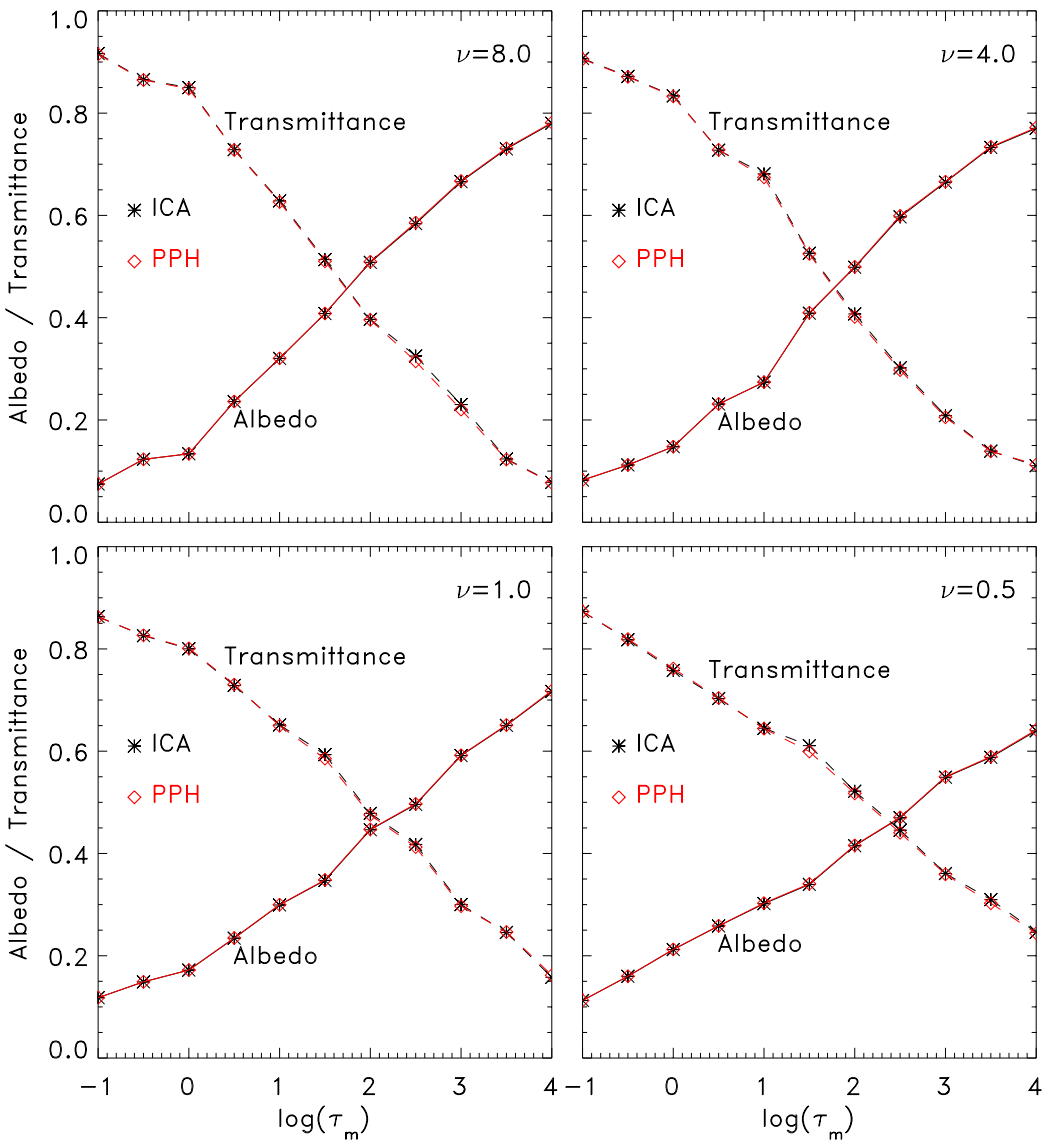


Fig. 9. As in Figure 4 but for broadband shortwave albedo and transmission and the same clouds as in Figure 8.

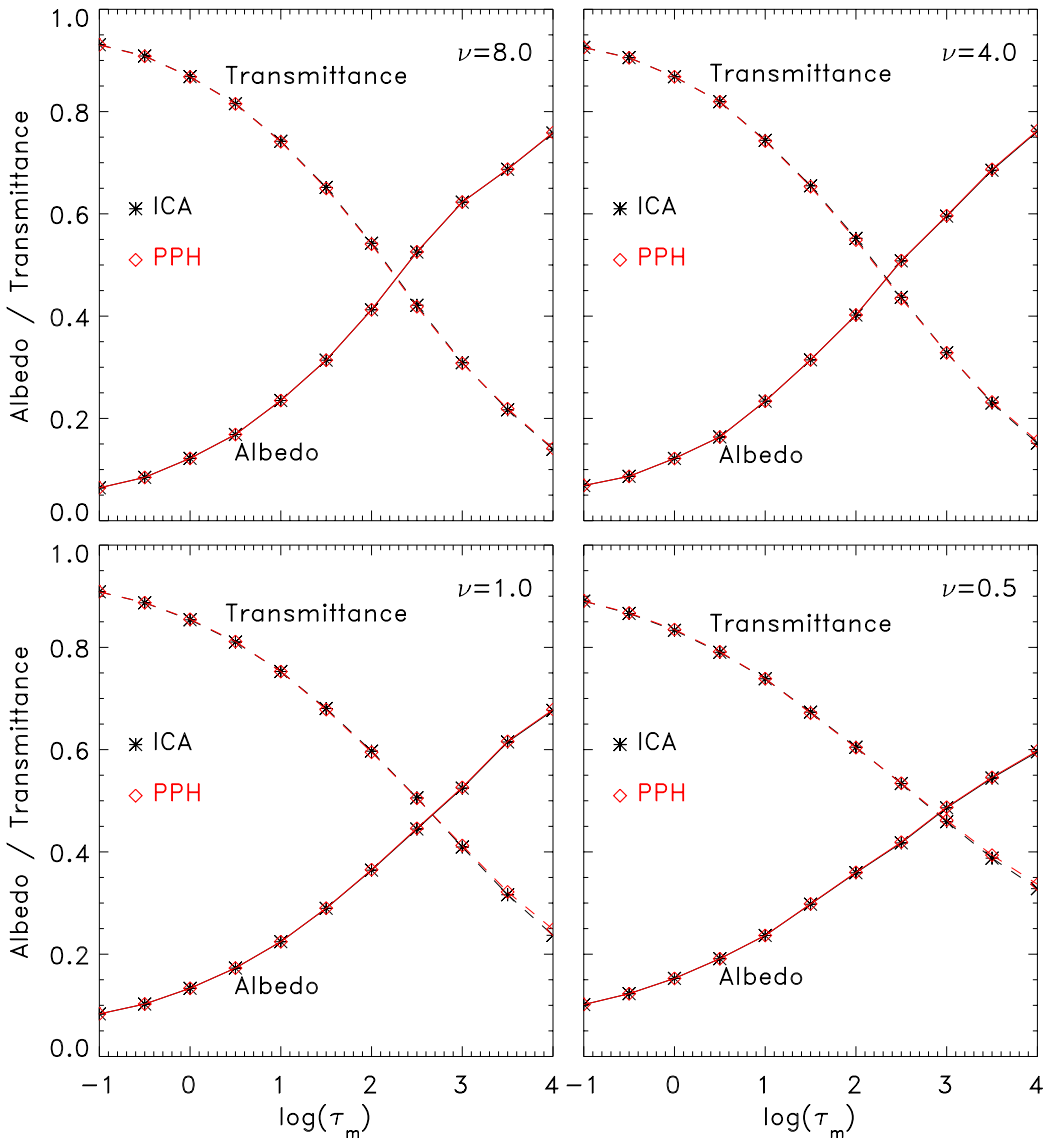


Fig. 10. As in Figure 9 except for water cloud only with particle size varies from  $7 \mu\text{m}$  to  $17 \mu\text{m}$ .

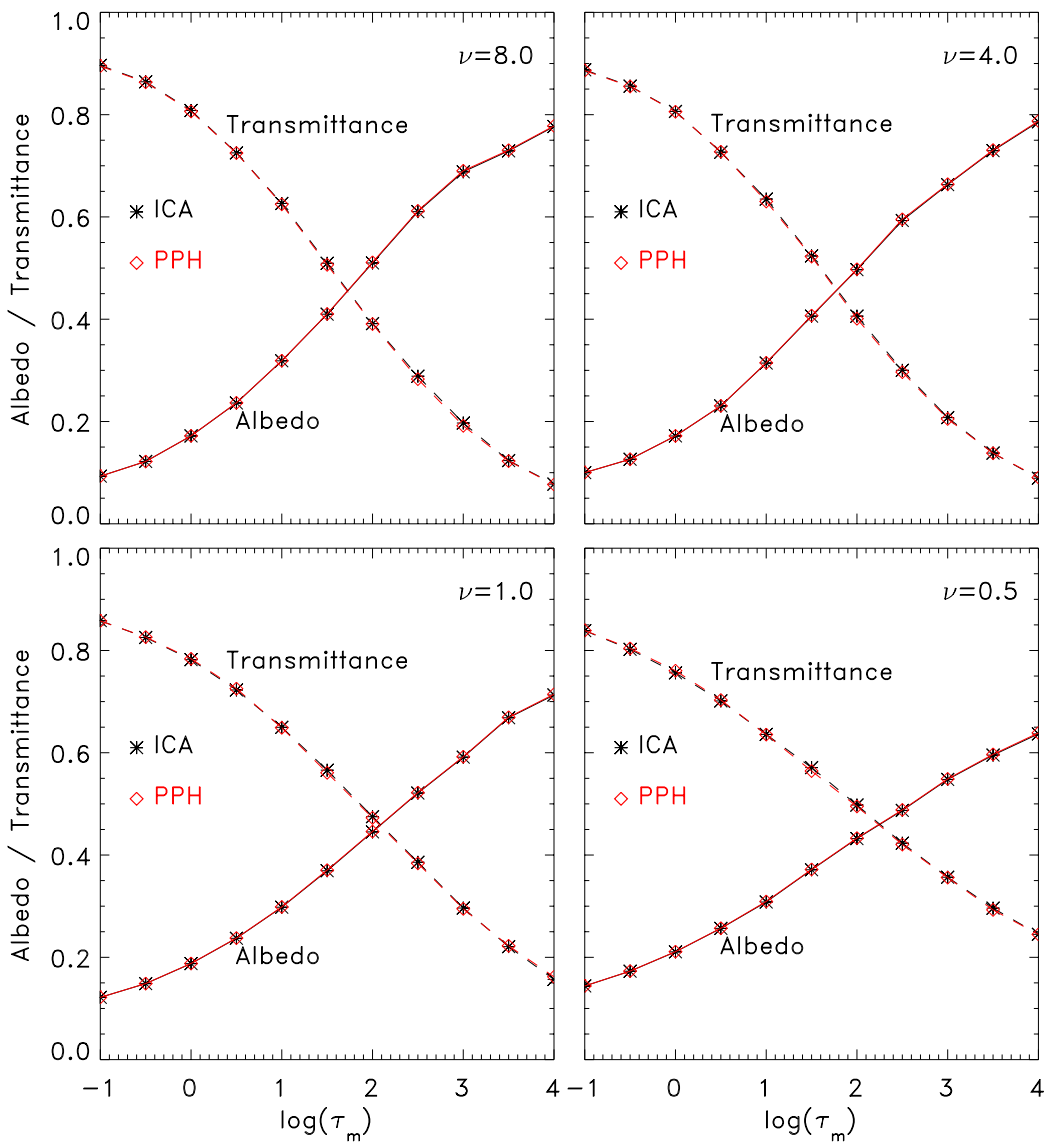


Fig. 11. As in Figure 9 except for ice cloud only with particle size varies from 17  $\mu\text{m}$  to 80  $\mu\text{m}$ .